Applied Physics B (2022) 128:53
https://doi.org/10.1007/s00340-022-07773-3

Applied Physics B
Lasers and Optics

Numerical analysis of reconstructed image of light-in-flight recording by holography with a magnifying optical system

Tomoyoshi Inoue[1,2] · Mika Sasaki[1] · Kenzo Nishio[3] · Toshihiro Kubota[4] · Yasuhiro Awatsuji[5]

Received: 29 December 2021 / Accepted: 25 January 2022 / Published online: 17 February 2022

Abstract
We analyze the distortions in the reconstructed images of light-in-flight recording by holography with a magnifying optical system. To analyze the distortions, we focused on a speed at which the light pulse sweeps the recording material. We developed a numerical simulation model based on the ray tracing method for this analysis. We simulated the reconstructed images by considering (1) the magnification of a magnifying optical system and (2) the sweeping speed of the object and reference light pulse. We found that the distortion becomes larger when we use a magnifying optical system with a higher magnification. In addition, the results of the numerical simulations showed that range, where the light pulse is recorded on the recording material, becomes narrow when the sweeping speed of the magnified object light pulse is not equal to that of the reference light pulse.

1 Introduction

In recent years, ultrashort laser pulses have a wide variety of applications for precise material processing, developing various kinds of super-resolution microscopy, revealing light–matter interactions [1–5], and so on. The uses of ultrashort light pulses for both fundamental research and its applications are increasing rapidly [6–8]. As these uses of ultrashort light pulses increase, observing the ultrashort light pulses becomes increasingly important. Among them, it is necessary to observe light pulse propagation or ultrafast phenomena induced by the propagating light pulse evolves in a microscopic region. For example, light–matter interaction, high-power plasmas induced by a femtosecond light pulse, and laser material processing typically evolving in a microscopic region. Therefore, an imaging technique for observing the magnified light pulse propagation is needed. Many researchers have reported techniques that enable us to record, visualize, and observe the behavior or properties of the propagating ultrashort light pulse and ultrafast phenomena caused by the ultrashort light pulses. Most of the techniques need a pulsed-light train or multiple exposures [9–12].

Among these techniques, optical holographic imaging has a huge impact on the observation of light pulse propagation. Light-in-flight recording by holography [13–25] is a powerful tool for recording and observing light pulse propagation in a microscopic region. This technique is able to record and reconstruct a propagating ultrashort light pulse as a spatially and temporally continuous motion picture. In addition, this technique can record of ultrashort light pulse propagation in a single shot. Furthermore, not only two-dimensional (2D) but also three-dimensional (3D) information of the propagating light pulse is obtained by the technique, because this technique is based on optical holography that records and reconstructs the intensity and phase of the light [17].

Even though latest ultrafast imaging techniques are developed, numerical simulation is common for studying light propagation in the macroscopic and microscopic region. The same is true for magnified light pulse imaging using

✉ Yasuhiro Awatsuji
awatsuji@kit.ac.jp

1 Graduate School of Science and Technology, Kyoto Institute of Technology, Matsugasaki, Sakyo-ku, Kyoto 606-8585, Japan

2 Japan Society for the Promotion of Science, Kojimachi Business Center Building, 5-3-1 Kojimachi, Chiyoda-ku, Tokyo 102-0083, Japan

3 Advanced Technology Center, Kyoto Institute of Technology, Matsugasaki, Sakyo-ku, Kyoto 606-8585, Japan

4 Kubota Holography Laboratory Corporation, Nishihata 34-1-609, Ogura-cho, Uji, Kyoto 611-0042, Japan

5 Faculty of Electrical Engineering and Electronics, Kyoto Institute of Technology, Matsugasaki, Sakyo-ku, Kyoto 606-8585, Japan

light-in-flight recording by holography. The main difficulty comes from the speed of the light and the low time-coherence of the ultrashort light pulse. During the recording process, the technique records an interference fringe, which is formed by an object light pulse and a reference light pulse. To record the interference fringes, the object light pulse and the reference light pulse need to arrive at the same time to recording material. When the incident angle of the illumination light pulse and that of the reference light pulse are equal, the speed at which the object light sweeps the recording material is equal to that at which the reference light sweeps the recording material. In addition, these speeds are called as the sweeping speed of the reference light pulse and the sweeping speed of the illumination light pulse, respectively. On the other hand, when the incident angle of the illumination light pulse and that of the reference light pulse are not equal, the sweeping speed of the reference light pulse and that of the illumination light pulse are not equal. Therefore, the place where the object light pulse sweeps the recording material is not constant against the place, where the reference light pulse sweeps the recording material. Consequently, the optical path length difference between the object light pulse and the reference light pulse is not constant with respect to the direction in which the reference light pulse sweeps the recording material. Namely, it can be said that the difference in the sweeping speed of each light pulse affects the optical path-length difference. Note that, the sweeping speeds are required to determine the optical path-length difference between the reference light pulse and the object light pulse. Therefore, an optical path-length difference between the reference light pulse and the object light pulse is an important factor to record and observe the propagating light pulse as a motion picture.

To observe a magnified image of light pulse propagation by the technique, a magnifying optical system is needed to introduce into the optical setup of light-in-flight recording by holography. Introducing a magnifying optical system changes the sweeping speeds of the object light pulse. Thus, the optical path-length difference between the reference light pulse and the object light pulse differs from the conventional recording process. However, the effects of difference in the sweeping speed of the reference light pulse and that of the object light pulse have not been reported yet [19]. Furthermore, in Ref. [24], a numerical simulation for a reconstructed image when recording with a single microscope objective is performed. However, in the previous study, the effects of the magnification of the magnifying optical system and the difference in sweeping speed on the reconstructed images have not been investigated. Therefore, in this study, we developed a numerical simulation model based on the ray tracing method to evaluate the effects of (1) the magnification of a magnifying optical system and (2) the difference in the sweeping speeds of the light pulses. In the numerical simulation, the ray tracing method was adopted to determine the optical path-length of the object light pulses passing through a magnifying optical system. We assumed that the magnifying optical system is an afocal system. Considering the use of a magnification optical system with low magnification and that with high magnification, we evaluate the shape of the magnified images of the light pulses under the following two situations: (1) the sweeping speed of the object light pulse is equal to that of the object light pulse. (2) the sweeping speed of the object light pulse is not equal to that of the object light pulse during the recording process with light-in-flight recording by holography.

2 Light-in-flight recording by holography

Light-in-flight recording by holography combines optical holography and ultrashort light pulses. In general, holography can record not only amplitude but also phase information of an object. On the other hand, in principle, light-in-flight recording by holography records a scattered light pulse as an object light pulse. When we record and reconstruct a scattered light pulse from an object, the phase image of the object becomes a random pattern. Therefore, the phase information of the object cannot be faithfully recorded with the current light-in-flight recording by holography.

The technique records interference fringes formed by a reference light pulse and an object light pulse. The reference light pulse is obliquely incident to the recording material. Similarly, the object light pulse is obliquely incident to the recording material, because a light pulse, which is called the illumination light pulse, obliquely illuminates a diffuser plate or a diffusive object. Because of the low time-coherence of the ultrashort light pulse, the interference fringes are formed only when and where both light pulses arrive simultaneously at the recording material. As a result, the spatial–temporal information of the propagating light pulse is recorded at different points along the lateral direction of the recording material. Figure 1a shows a basic recording arrangement of light-in-flight recording by holography. The technique uses ultrashort light pulse from the ultrashort-pulsed laser to record a hologram. An ultrashort light pulse from an optical source is divided into two light pulses by a beam splitter. One light pulse is collimated and obliquely incident to a diffuser plate contacted with an object or a diffusive object. This light pulse is called as an illumination light pulse. The diffused or scattered light pulse irradiates the recording material. This light pulse is called as an object light pulse. The other light pulse is also obliquely incident to the recording material. This light pulse is called as a reference light pulse. Only when and where the object light pulse and the reference light pulse arrive at the recording material at the same time, interference fringes are formed by these

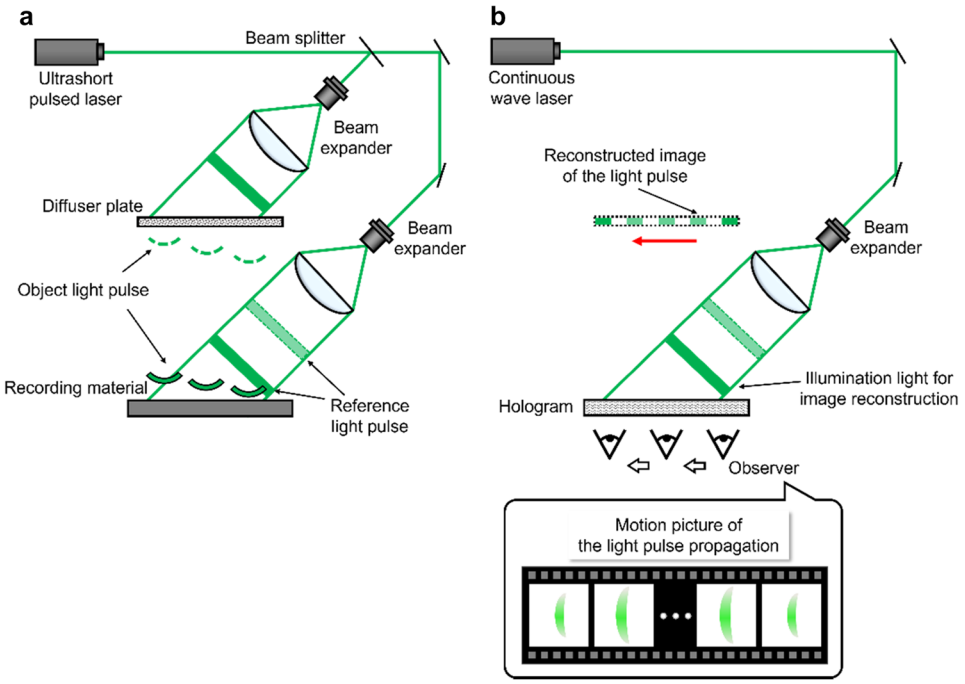

Fig. 1 Schematic diagram of the basic arrangement of light-in-flight recording by holography. **a** Recording. **b** Reconstruction

light pulses and recorded on the image sensor. Because the reference light pulse is incident to the recording material obliquely, the reference light pulse sweeps and crosses the recording material laterally. Therefore, the behavior of the light pulse propagating on the diffuser plate contacted with object or the diffusive object at each moment is recorded in each different part along the lateral direction of the recording material.

Figure 1b shows a schematic diagram of the image reconstruction process of the light-in-flight recording by holography. In the process, a continuous wave laser beam is obliquely incident to the hologram with the incident angle that is the same angle of the reference light pulse. We can observe the behavior of the propagating light pulse as a spatially and temporally continuous motion picture when we shift the observation point on the hologram laterally.

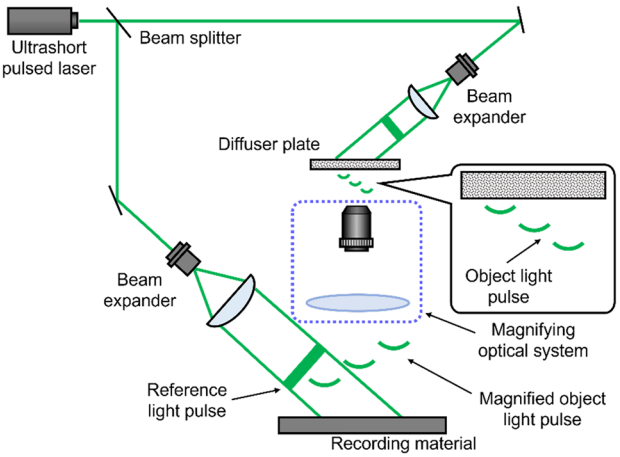

Fig. 2 Schematic illustration of the top view of light-in-flight recording by holography with a magnifying optical system

3 Light-in-flight recording by holography including a magnifying optical system

3.1 Schematic illustration

Figure 2 shows the schematic illustration of light-in-flight recording by holography with a magnifying optical system. The magnifying optical system is introduced to the conventional recording arrangement of light-in-flight recording by holography. We consider an afocal optical system as the magnifying optical system. Because the magnification is constant, it is easy to observe the image. The afocal optical system is placed between the diffuser plate and the recording material. The magnification of the optical system M is given by

$$M = -\frac{f_2}{f_1}, \tag{1}$$

where f_1 and f_2 are the focal length of the microscope objective and that of the plano-convex lens. After passing through the magnifying optical system, the object light pulse generated from the diffuser plate is inverted vertically and horizontally. Therefore, the reference light pulse and the

illumination light pulse are obliquely incident on the recording material and the diffuser plate in the opposite directions to each other, as shown in Fig. 2.

3.2 Sweeping speed of the light pulse: the speed at which the light pulse sweeps the recording material

We explain the speed at which a light pulse sweeps a recording material in light-in-flight recording by holography. In the recording process, interference fringes are formed and recorded by the recording material only when both light pulses arrive at the recording material simultaneously due to the short temporal coherence length of the ultrashort light pulse. In other words, to form the interference fringes, an optical path-length difference between the reference light pulse and the object light pulse is needed to be less than or equal to the temporal coherence length of the ultrashort light pulse. The optical path-length difference between the reference light pulse and the object light pulse is determined by the sweeping speed of the reference light pulse and that of the object light pulse.

We describe the sweeping speed of the reference light pulse and that of the object light pulse. These sweeping speeds are mainly determined by the incident angle of the light pulses as shown below. The sweeping speed of the reference light pulse v_r is given by

$$v_r = \frac{c}{\sin\theta_r}, \tag{2}$$

where c and θ_r are the speed of the light in the air and the incident angle of the reference light pulse, as shown in Fig. 3a. Similarly, the sweeping speed of the illumination light pulse v_i is also given by

$$v_i = \frac{c}{\sin\theta_i}, \tag{3}$$

where c and θ_i are the speed of the light in the air and the incident angle of the illumination light pulse to a diffuser plate, as shown in Fig. 3b. In a conventional optical system of light-in-flight recording by holography, we set the incident angle of the illumination light pulse to be equal to the incident angle of the reference light pulse [23]. As a result, the sweeping speed of the object light pulse is equal to the speed at which the illumination light pulse sweeps the diffuser plate. Thus, the sweeping speed of the object light pulse is equal to that of the illumination light pulse in general. Then, we can express the sweeping speed of the object light pulse is as

$$v_o = v_i. \tag{4}$$

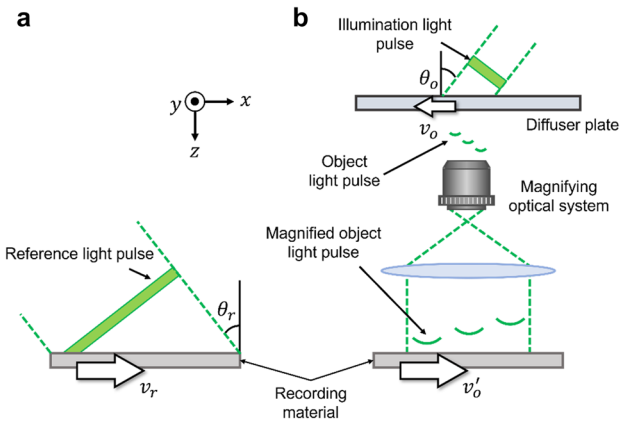

Fig. 3 Diffuser plate and the recording material of the recording arrangement of light-in-flight recording by holography with a magnifying optical system. **a** Reference light pulse. **b** Object light pulse

However, after passing through the magnifying optical system, the sweeping speed of the magnified object light pulse v'_o is given by

$$v'_o = M \times v_o = M \times v_i = \frac{M \times c}{\sin\theta_i}, \tag{5}$$

where M is the magnification of the magnifying optical system. When recording the object light pulse, it is necessary that the sweeping speed of the reference light pulse is equal to that of the object light pulse in the x direction according to the principle of light-in-flight recording by holography. However, introducing the magnifying optical system to the optical arrangement changes the sweeping speed of the object light pulse as seen from Eq. (5). As a result, when introducing the magnifying optical system, the sweeping speed of the object light pulse is faster than that of the conventional one. The arrival time of the object light pulse changes, because the sweeping speed of the object light pulse changes, that is, the place where the object light pulse sweeps the recording material is not constant against the place where the reference light pulse sweeps the recording material. Thus, the optical path-length difference between the object light pulse and the reference light pulse is not constant with respect to the direction in which the reference light pulse sweeps the recording material. Consequently, the place where the interference fringes are formed is different from that of the conventional recording process.

4 Simulation model

To investigate the effect of the difference in the sweeping speed of the object light pulse on a magnified image of light pulse propagation, we developed a numerical

simulation model of light-in-flight recording by holography including a magnifying optical system. The numerical simulation model is based on the ray tracing method. We numerically simulate the magnified images of light-in-flight recording by holography with the magnifying optical system. Figure 4a schematically shows the simulation model. We consider the simulation model on the basis of the optical configuration, as shown in Fig. 3b. We defined the plane on which the diffuser plate was set and the optical axis that was perpendicular to the diffuser plate as the xy plane and z-axis, respectively. The optical path-length of the object light pulse is calculated by the ray tracing method. We define coordinates of points and parameters in Fig. 4a, as shown in Tables 1 and 2. In the numerical simulation, the following conditions were assumed and applied for calculation simplicity.

1. An object light pulse scattered at O propagates in the z -direction. After passing through the magnifying optical system, an object light pulse scattered at O is recorded at R_O. The object light pulse and the reference light pulse simultaneously arrive at R_O. Interference fringes are generated at R_O, because the optical path-length of the reference light pulse is equal to that of the object light pulse.
2. The cross section of the illumination light pulse and the diffuser plate are linear.
3. The cross section of the reference light pulse and the recording material are linear.
4. The diffuser plate and the recording material are placed parallel to each other.
5. The refractive index and thickness of the glass material of the lenses are not considered.
6. We set the light pulse to be isotropically scattered from the surface of the diffuser.
7. Light-in-flight recording by holography typically records a scattered object light pulse as a Fresnel hologram. Therefore, to assume the scattered light pulse in the Fresnel propagation, the diffuser plate and the recording material are not placed in the input plane and the output plane of the 4f-system (the magnifying optical system), respectively.

When any parameters of l_1, l_2, f_1, f_2, and M are given, the other parameters are determined. Thus, parameters, namely, d_1, d_2, W, n, θ_o, θ_r, and l_1, l_2, f_1, f_2, and M, should be given in the numerical simulation. To calculate the image of the propagating light pulse recorded at the set of R whose y-coordinate is zero on the recording material, as shown in Fig. 4a, we calculate the set of points on the diffuser plate. The object light pulse occurring at a certain point A arrives at R through L_1 and L_2, which are points in Lens 1 and Lens 2. Then, $t_{A-L_1-L_2-R}$, which is the time required for the object light pulse to propagate $A \rightarrow L_1 \rightarrow L_2 \rightarrow R$, is given as

$$t_{A-L_1-L_2-R} = \frac{\overline{AL_1}}{c} + \frac{\overline{L_1L_2}}{c} + \frac{\overline{L_2R}}{c}. \tag{6}$$

Here, c is the speed of light in the air, $\overline{AL_1}$, $\overline{L_1L_2}$, and $\overline{L_2R}$ are the optical path-length from A to L_1, the optical path-length from L_1 to L_2, and the optical path-length from L_2 to R, respectively. In addition, the time when the object light pulse occurs at A and the time when the object light pulse arrives at R are defied as T_A and T_R, respectively. The time when the object light pulse arrives at R is expressed as

$$T_R = T_A + t_{A-L_1-L_2-R}. \tag{7}$$

A_x and A are located on the same pulse front at the time T_A. We consider the case in which the illumination light pulse propagates on the diffuser plate and the object light pulse occurs at O at time T_o. Because the illumination light pulse is incident on the diffuser plate at the incident angle θ_i against the normal of the diffuser plate, the sweeping speed of the illumination light pulse is given by Eq. (3). Then, $t_{A_x\text{-}O}$, which is the required time for the illumination light pulse to propagate the diffuser plate from O to A_x, is given as

$$t_{A_x\text{-}O} = \frac{\overline{OA_X}}{v_i}. \tag{8}$$

Since $\overline{OA_x}$ is the optical path-length from O to A_x, T_o is given as

$$T_O = T_A + t_{A_x\text{-}O}. \tag{9}$$

In addition, t_{O-R_o}, which is the time required for the object light pulse to propagate from O to R_O through the principal point of Lens 1 and Lens 2, is given by

$$t_{O\text{-}R_o} = \frac{\overline{OR_O}}{c}. \tag{10}$$

Here, $\overline{OR_O}$ is the optical path-length from O to R_O. As a result, the time T_{R_o} when the object light pulse occurs at O arrives R_O is given as

$$T_{R_o} = T_O + t_{O\text{-}R_o} = T_A + t_{A_x\text{-}O} + t_{O\text{-}R_o}. \tag{11}$$

Considering the condition [1], the time τ_{R_O} when the reference light pulse arrives R_O is expressed by

$$\tau_{R_O} = T_{R_O}. \tag{12}$$

Because the reference light pulse is incident on the recording material at the incident angle θ_r against the surface of the recording material, the sweeping speed of the reference light pulse is given by Eq. (2). In addition, t_{R-R_O}, which

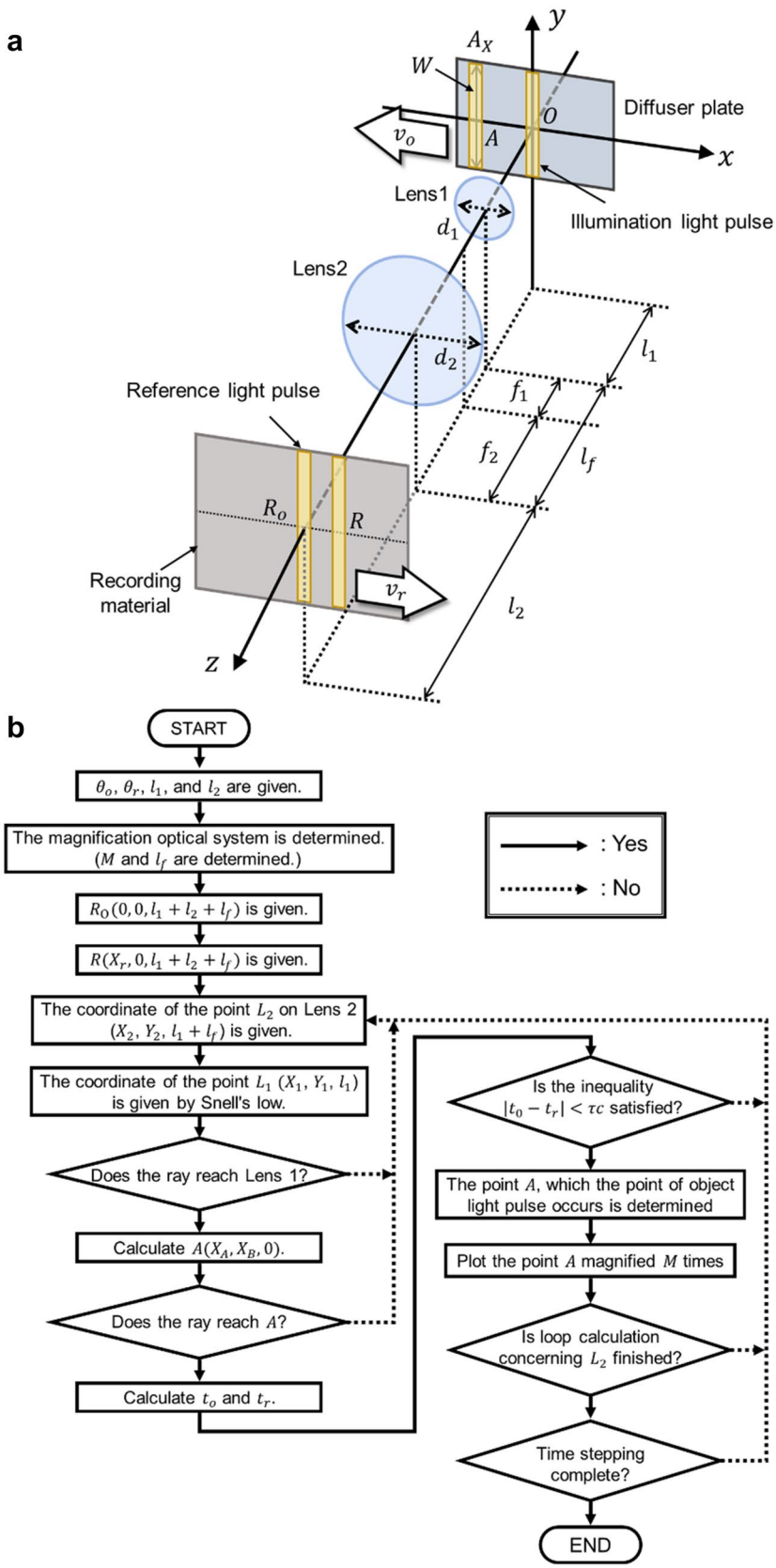

Fig. 4 Schematic illustration of the simulation model. **a** Recording process of light-in-flight recording by holography with a magnifying optical system. **b** Flowchart of the numerical simulation

Table 1 Definition of coordinates of points

Coordinates of Points	Definition
O (0, 0, 0)	Origin of *xyz*-coordinates
R_O (0, 0, l_1+l_f+l_2)	Cross point between z-axis and the recording material
R (X_r, 0, l_1+l_f+l_2)	Observation point on the recording material
A (X_A, Y_A, 0)	Point on the diffuser plate
A_x (X_A, 0, 0)	Point, whose x-coordinate corresponds to A, on the diffuser plate
L_1 (X_1,Y_1,l_1)	A point on the principal plane of Lens 1
L_2(X_2,Y_2,l_1+l_f)	A point on the principal plane of Lens 2

Table 2 Definition of parameters

Parameters	Definition
θ_o	Incident angle of the illumination light pulse against the normal of the diffuser plate
θ_r	Incident angle of the reference light pulse against the normal of the recording material
l_1	Distance between the diffuser plate and Lens 1
l_2	Distance between the recording material and Lens 2
l_f	Distance between Lens 1 and Lens 2
f_1	Focal length of Lens 1
f_2	Focal length of Lens 2
d_1	Aperture diameter of Lens 1
d_2	Aperture diameter of Lens 2
M	Magnification of the reconstructed image
W	Beam diameter of the illumination light pulse
n	Number of the rays
τ	Pulse duration of the ultrashort light pulse
c	Speed of the light in the air

is the time required for the reference light pulse to propagate from R to R_O, is given by

$$t_{R-R_O} = \frac{\overline{RR_O}}{v_R}. \tag{13}$$

Here, $\overline{RR_O}$ is the optical path-length from R to R_O. Then, the time τ_R when the reference light pulse reaches R_O after passing R is expressed by

$$\tau_R = \tau_{R_O} - t_{R-R_O} = T_{R_O} - t_{R-R_O}. \tag{14}$$

When the object light pulse occurred at A arrives at R, the reference light pulse arrives at R simultaneously. By applying Eqs. (6)–(14), we obtain the following equation:

$$\frac{\overline{AL_1}}{c} + \frac{\overline{L_1L_2}}{c} + \frac{\overline{L_2R}}{c} - \frac{\overline{OA_X}}{v_i} - \frac{\overline{OR_O}}{c} = \frac{\overline{RR_O}}{v_R}. \tag{15}$$

If Eq. (15) is satisfied, the object light pulse containing the information on A is recorded at R. In the numerical simulation, we consider the following condition:

$$\left| \frac{\overline{AL_1}}{c} + \frac{\overline{L_1L_2}}{c} + \frac{\overline{L_2R}}{c} - \frac{\overline{OA_X}}{v_i} - \frac{\overline{OR_O}}{c} - \frac{\overline{RR_O}}{v_R} \right| < \tau c. \tag{16}$$

Equation (16) shows that the light pulse occurred at A is recorded at R when the optical path-length difference between the object light pulse and the reference light pulse is shorter than the temporal coherence length of the ultrashort pulse.

Figure 4b shows the flowchart of the numerical simulation. By varying the coordinate of the observation point R and conducting the same calculation mentioned above, we obtain a set of points on the diffuser plate that scatters the object light pulse recorded at R in the form of an interference fringe. When the coordinate of A is found, we plot a point of A magnified M times. Thus, we can observe the reconstructed image of the magnified light pulse recorded by light-in-flight recording by holography with a magnifying optical system.

5 Simulation parameters

First, we performed a numerical simulation of the reconstructed images using a magnifying optical system with a lower magnification. We simulated the reconstructed images under the following two parameters: (1) the sweeping speed of the object light pulse is equal to that of the object light pulse in the x direction. (2) the sweeping speed of the object light pulse is not equal to that of the object light pulse in the x direction.

By considering the two situations mentioned above, we set the two simulation parameters: (1) the sweeping speed of the object light pulse is equal to that of the reference light pulse. (2) the sweeping speed of the object light pulse is seven times faster than that of the reference light pulse. The two conditions are shown in Tables 3 and 4, respectively.

Second, we also performed a numerical simulation of the reconstructed images using a magnifying optical system with a higher magnification. Similarly, we set the two simulation parameters with the higher magnification: (3) the sweeping speed of the object light pulse is equal to that

Table 3 Simulation parameters for Condition (1)

Parameters	Values
θ_o	75.4°
θ_r	14°
l_1	3 cm
l_2	10 cm
l_f	10 cm
f_1	2 cm
f_2	8 cm
d_1	1 cm
d_2	4 cm
M	7.78
W	10 cm
n	50,000
τ	178 fs
c	3.0×10^8 m/s

Table 4 Simulation parameters for Condition (2)

Parameters	Values
θ_o	14°
θ_r	14°
l_1	3 cm
l_2	10 cm
l_f	10 cm
f_1	2 cm
f_2	8 cm
d_1	1 cm
d_2	4 cm
M	7.78
W	10 cm
n	50,000
τ	178 fs
c	3.0×10^8 m/s

Table 5 Simulation parameters for Condition (3)

Parameters	Values
θ_o	38°
θ_r	2°
l_1	1.5 cm
l_2	20 cm
l_f	16.9 cm
f_1	0.9 cm
f_2	16 cm
d_1	1.2 cm
d_2	6 cm
M	17.8
W	10 cm
n	50,000
τ	178 fs
c	3.0×10^8 m/s

Table 6 Simulation parameters for Condition (4)

Parameters	Values
θ_o	2°
θ_r	2°
l_1	1.5 cm
l_2	20 cm
l_f	16.9 cm
f_1	0.9 cm
f_2	16 cm
d_1	1.2 cm
d_2	6 cm
M	17.8
W	10 cm
n	50,000
τ	178 fs
c	3.0×10^8 m/s

of the reference light pulse. (4) the sweeping speed of the object light pulse is 17-times faster than that of the reference light pulse. The two conditions are shown in Tables 5 and 6, respectively.

In this study, to conduct the numerical simulation effectively, we determined "the number of rays that pass through the lens 2" as the total number of rays n. In the numerical simulation, there are many rays that can reach the diffuser plate from a certain point of the recording material. Therefore, when calculating all paths of rays, the number of rays needed to be calculated becomes very large, and the calculation efficiency also decreases. Figure 5 schematically shows the result of plotting the rays in the lens 2 under Condition (1). The small dots represent the points, where the rays passed through lens 2. As you can see, we could calculate all rays that pass through the lens 2. Therefore, we consider that the number of rays in this study is reasonable. In addition, we consider that enough number of rays is related to the diameter of a tube lens (lens 2).

6 Results and discussion

Figures 6 and 7 show the simulation results in the case of a lower magnification. The x- and y-axes of the simulation results correspond to those in Fig. 4a. Small dots represent calculated points of the magnified object light pulse. The magnified images are represented by a set of calculated points. Figures 6 shows the simulation result under Condition (1). We obtained the simulation results by changing the observation area from − 2 to 2 cm by 0.1 cm (see Video 1, Supplementary materials). We do not show all the results but choose results at a certain interval. From Fig. 6a–f, X_r changed as follows. a: − 0.4, b: − 0.2,

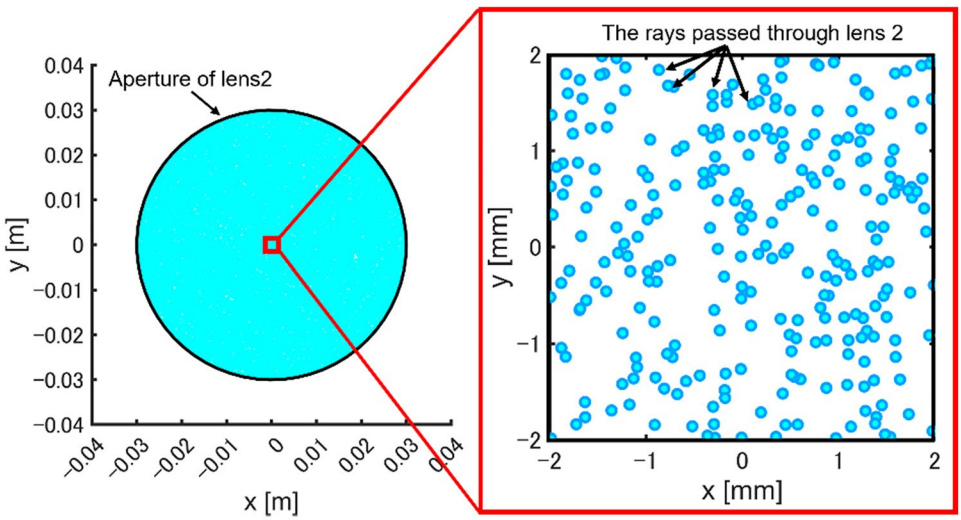

Fig. 5 Rays in the lens 2

c: − 0.0, d: 0.2, e: 0.4, and f: 0.6 cm. Figure 6g shows a circular reconstructed image with the largest diameter in the numerical simulation under Condition (1). The circle was calculated by applying the least squares method to the calculated plots of the magnified object light pulse. In this result, the diameter of the circle is 1.08 cm. Figure 6h shows the range in which the magnified object light pulse propagates on the image plane. The small green dots represent the reconstructed image that first appeared in the motion picture of light pulse propagation. The small blue dots represent the last observed reconstructed image right before the reconstructed image disappeared in the motion picture. We found that the magnified object light pulse propagates 0.53 cm.

Similarly, Fig. 7 shows the simulation results under Condition (2). As mentioned above, we obtained the simulation results by changing the observation area from − 2 to 2 cm by 0.1 cm (see Video 2, Supplementary materials). From Fig. 7a, b, X_r changed as follows. a: −0.4, b: −0.2, c: −0 .0, d: 0.2, e: 0.4, and f: 0.6 cm. Figure 7g shows a circular reconstructed image with the largest diameter in the numerical simulation under Condition (2). Same as above, the circle was calculated by applying the least squares method to the calculated plots of the magnified object light pulse. As a result, the diameter of the circle is 0.74 cm. Figure 7h shows the range in which the magnified object light pulse propagates on the image plane. The small green dots represent the reconstructed image that first appeared in the motion picture of light pulse propagation. The small blue dots represent the last observed reconstructed image right before the reconstructed image disappeared in the motion picture. We found that the magnified object light pulse propagates 0.27 cm. We can observe the magnified image of the light pulse propagation when X_r, the observation points on the hologram, changes.

Figure 8 shows the simulation results under Condition (3). We obtained the simulation results by changing the observation area from − 2 to 2 cm by 0.1 cm (see Video 3, Supplementary materials). We do not show all the results but choose results at certain intervals. From Fig. 8a–f, X_r changed as follows. a: −0.4, b: −0.2, c: −0.0, d: 0.2, e: 0.4, f: 0.6, g: 0.8, and h: 1.0 cm. Figure 8i shows a circular reconstructed image with the largest diameter in the numerical simulation under Condition (3). The circle was calculated by applying the least squares method to the calculated plots of the magnified object light pulse. The diameter of the circle is 5.5 cm. Figure 8j shows the range in which the magnified object light pulse propagates on the image plane. The small green dots represent the reconstructed image that first appeared in the motion picture of light pulse propagation. The small blue dots represent the last observed reconstructed image right before the reconstructed image disappeared in the motion picture. We found that the magnified object light pulse propagates 2.13 cm.

Similarly, Fig. 9 shows the simulation results under Condition (4). As mentioned above, we obtained the simulation results by changing the observation area from − 2 to 2 cm by 0.1 cm (see Video 4, Supplementary materials). From Fig. 9a–g, X_r changed as follows. a: −0.4, b: −0.2, c: −0.0, d: 0.2, e: 0.4, f: 0.6, g: 0.8, and h: 1.0 cm. We can observe the magnified image of the light pulse propagation when X_r, the observation points on the hologram, changes. Figure 9i shows a circular reconstructed image with the largest diameter in the numerical simulation under Condition (4). The circle was calculated by applying the least squares method to the calculated plots of the magnified object light pulse. The diameter of the circle is 2.3 cm. Figure 9j shows the range in which the magnified object light pulse propagates on the image plane. The small green dots represent the reconstructed image that first appeared in the motion picture

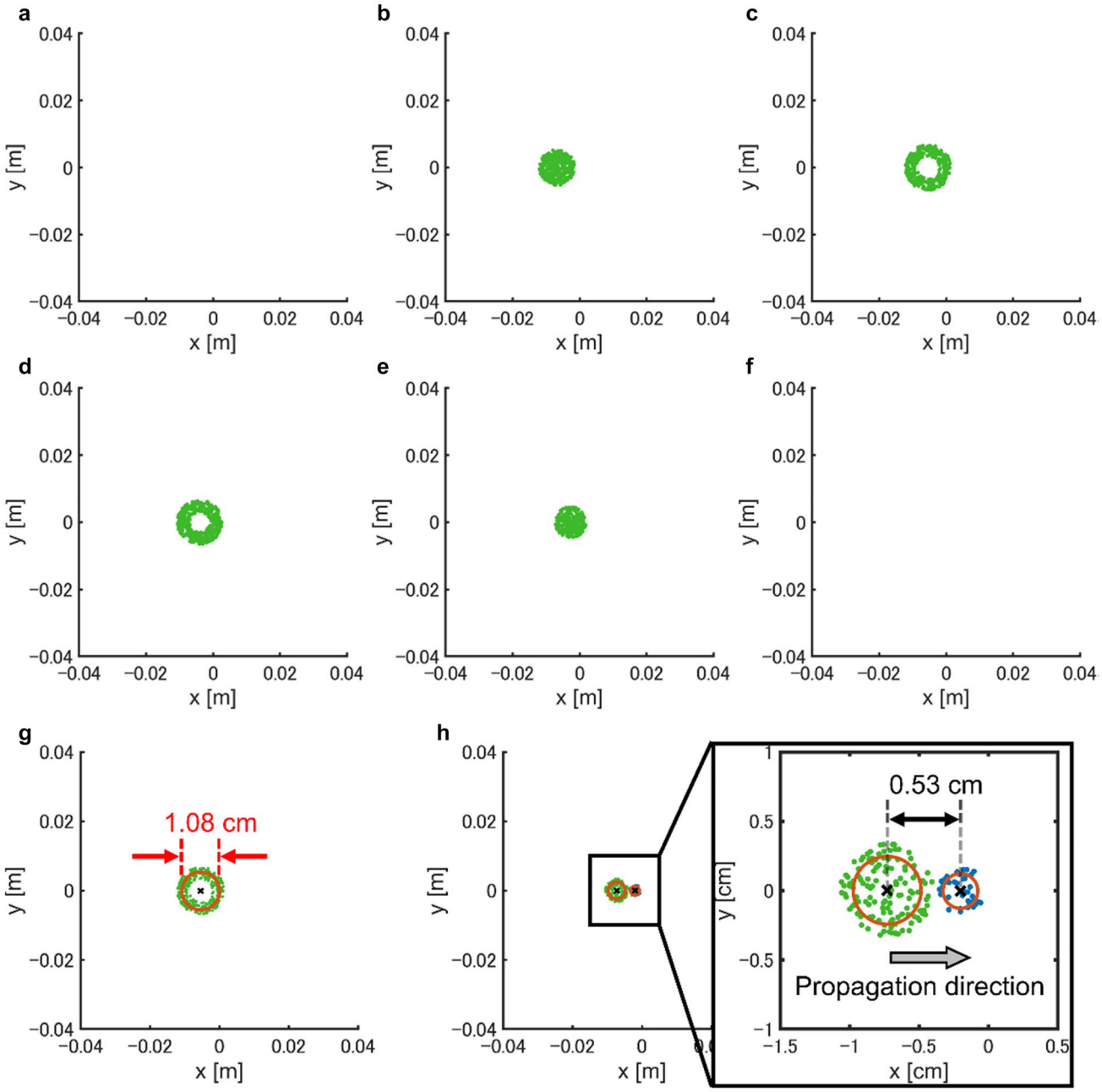

Fig. 6 Simulation results of the magnified light pulse propagation under Condition (1). **a** $X_r = -0.4$, **b** −0.2, **c** 0.0, **d** 0.2, **e** 0.4, **f** 0.6 (see Video 1, Supplementary materials). **g** Circular reconstructed image with the largest diameter. **h** Range in which the magnified object light pulse propagates on the image plane

of light pulse propagation. The small blue dots represent the last observed reconstructed image right before the reconstructed image disappeared in the motion picture. We found that the magnified object light pulse propagates 1.09 cm.

Here, we discuss the simulation results. We could observe circular or arcuate distortions in the results. In the previous study, similar circular or arcuate distortions have been observed in the numerical simulation for light-in-flight recording by holography with a magnifying optical system [16, 23]. These distortions arise, because the optical path length difference between the reference and the object light pulse is geometrically determined. We understand that the numerical results show that the shape of the reconstructed images was affected by (1) the magnification of the magnifying optical system and (2) the difference in the sweeping speed between the reference light pulse and the object light pulse. First, we examined the effect of the magnification of the magnifying optical system on the

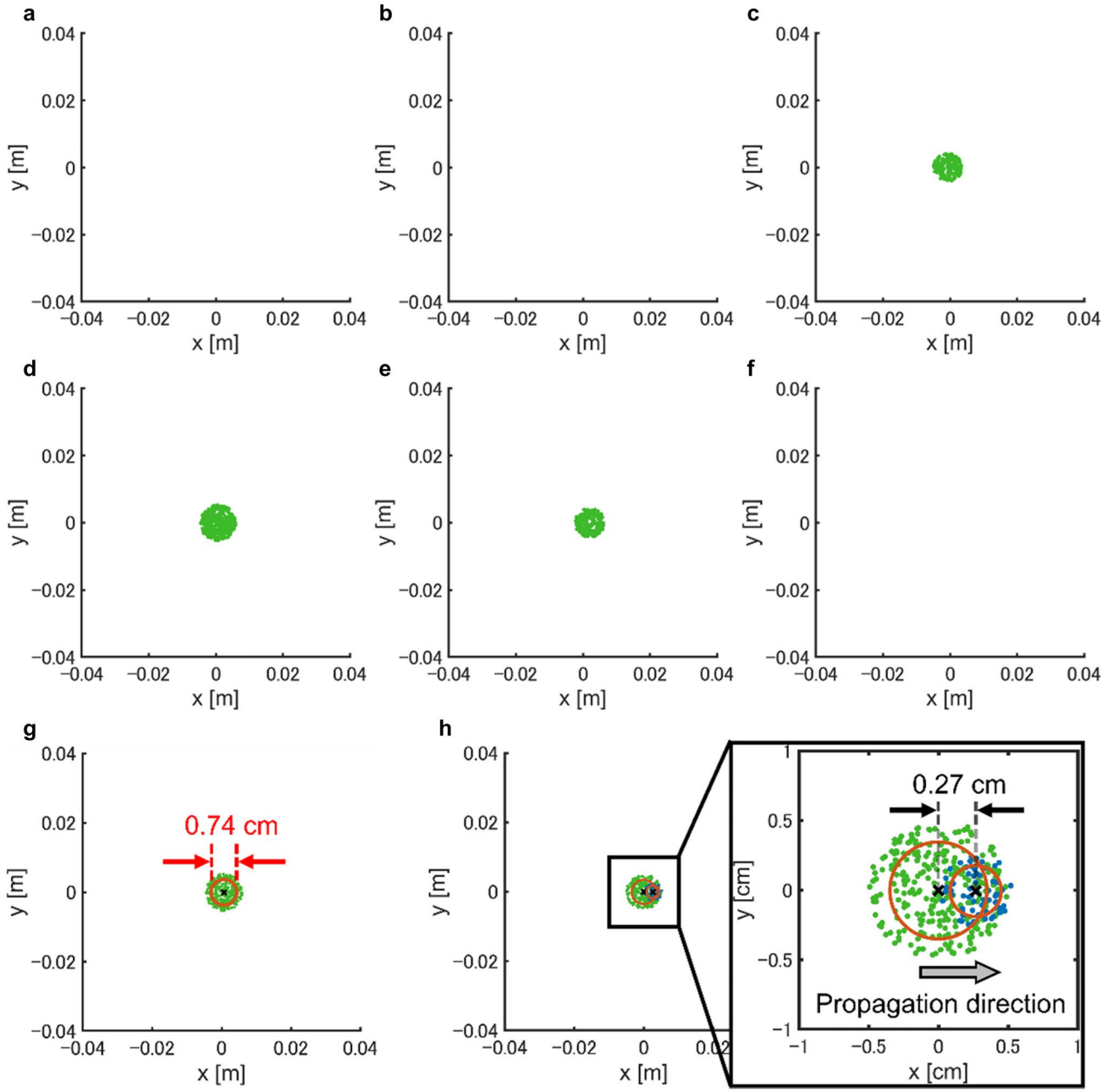

Fig. 7 Simulation results of the magnified light pulse propagation under Condition (2). **a** $X_r = -0.4$, **b** −0.2, **c** 0, **d** 0.2, **e** 0.4, **f** 0.6 (see Video 2, Supplementary materials). **g** Circular reconstructed image with the largest diameter. **h** Range in which the magnified object light pulse propagates on the image plane

reconstructed images. Figures 8 and 9 show the circular distortion of the image of the light pulse becomes large in the case of Condition (3) and (4). These results show that the distortion of the reconstructed images occurs when we use a magnifying optical system with a higher magnification. Second, we examined the effect of the difference in the sweeping speed between the light pulses on the reconstructed images. Comparing Figs. 8, 9, the diameter of the reconstructed images becomes larger when the sweeping speed of the object light pulse is equal to that of the reference light pulse.

We also discussed a range of the recording material that can record interference fringes, because the magnified image of the propagating light pulse at each moment is recorded at different points along the direction of reference light pulse propagation. The image of the object light pulse did not appear in several frames of the simulation results. The object light pulse could not be recorded, because there was

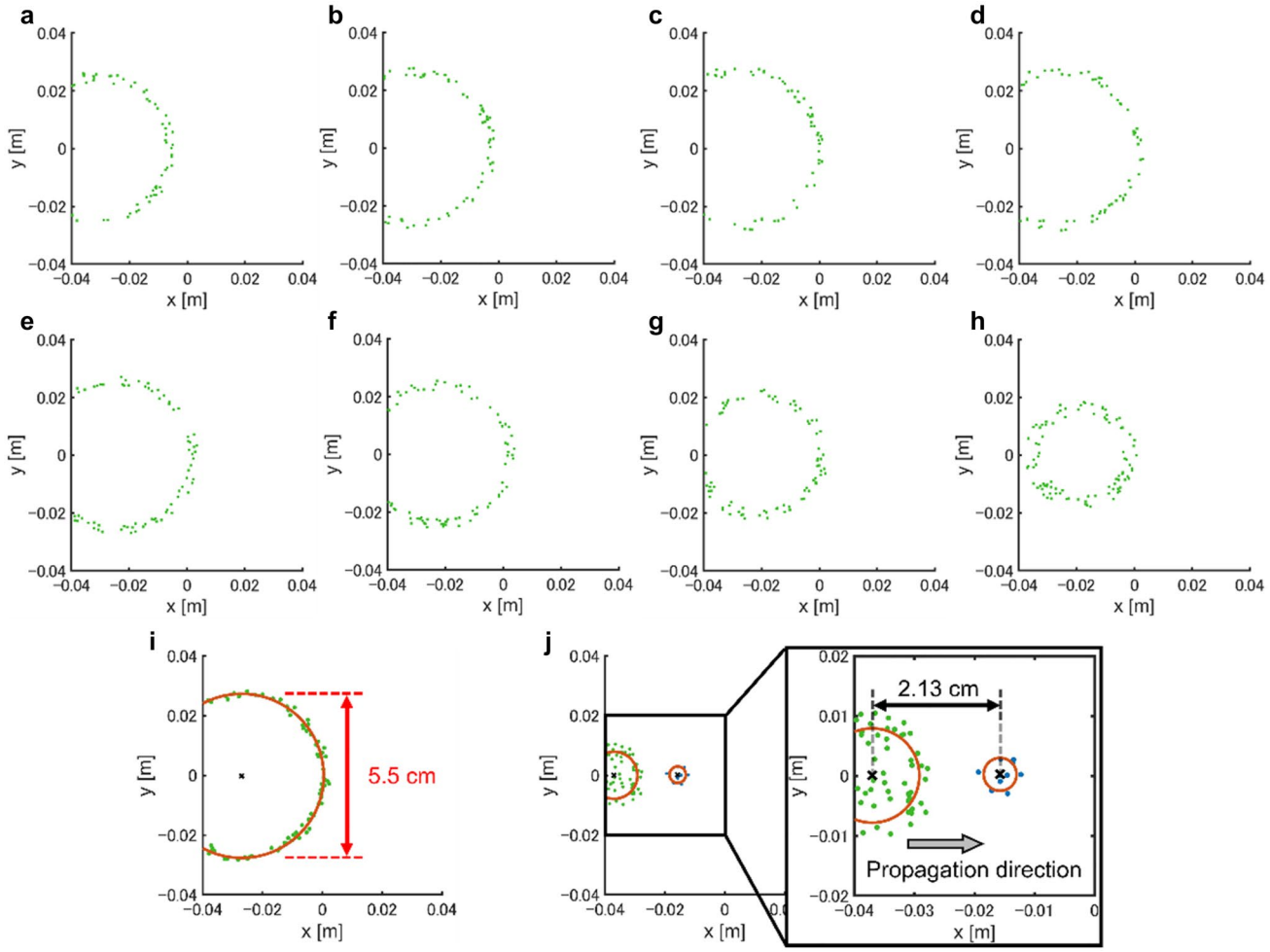

Fig. 8 Simulation results of the magnified light pulse propagation under Condition (3). **a** $X_r = -0.4$, **b** −0.2, **c** 0, **d** 0.2, **e** 0.4, **f** 0.6, **g** 0.8, **h** 1.0 mm (see Video 3, Supplementary materials). **i** Circular reconstructed image with the largest diameter. **j** Range in which the magnified object light pulse propagates on the image plane

no light ray satisfying Eq. (16). To discuss the simulation results, we also examined the effect of the magnification of the magnifying optical system on the reconstructed images. Comparing Figs. 8j, 9j, the range in which the light pulse propagates on the image plane in Condition (4) is about half as long as that of Condition (3). Considering the recording time of the magnified light pulse, the simulation results of Condition (4) show that the recording time of the motion picture of the magnified light pulse is decreased. Regardless of the magnification, the range where the light pulse is recorded on the recording material becomes narrow when the sweeping speed of the magnified object light pulse is not equal to that of the reference light pulse. This is because the optical path length difference between the object light pulse and the reference light pulse increases as the difference in sweeping speed between both light pulses increases.

From these results, the difference in sweeping speed between the reference light pulse and the object light pulse directly affects the shape of the magnified images of the light pulse and a range of the recording material that can record interference fringes. In addition, our result indicates that the higher the magnification of the magnifying optical system, the larger the distortion of the magnified image and the decrease of the range. It can be seen from the results that a compensation method for distortions is required to accurately observe the magnified images of the light pulse when introducing the magnifying optical system into light-in-flight recording by holography to observe the magnified light pulse. We are studying compensation methods using the results obtained by our numerical simulation model. We will investigate the numerical analysis of the images as a future work.

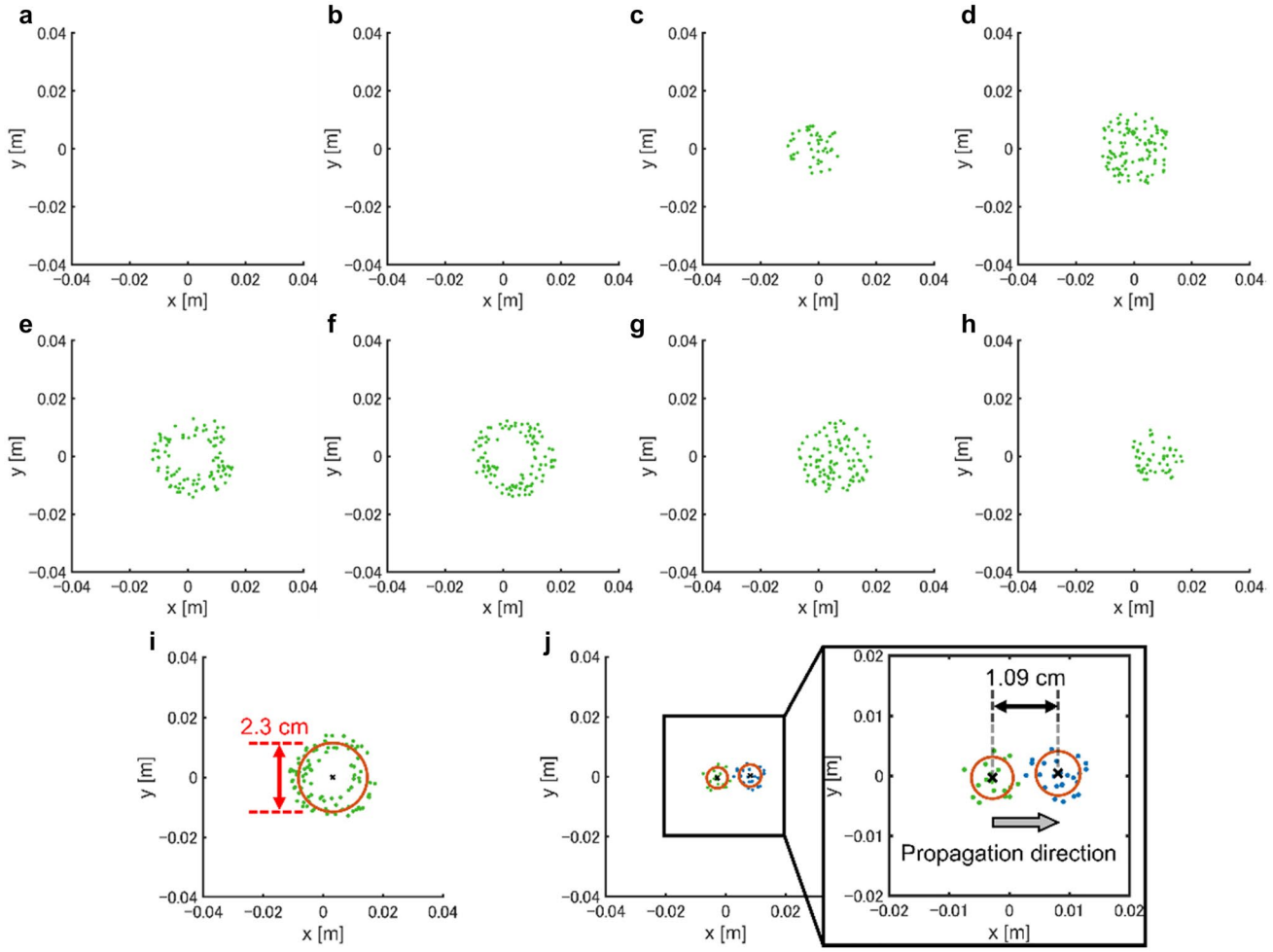

Fig. 9 Simulation results of the magnified light pulse propagation under Condition (4). **a** $X_r = -0.4$, **b** −0.2, **c** 0, **d** 0.2, **e** 0.4, **f** 0.6, **g** 0.8, **h** 1.0 mm (see Video 4, Supplementary materials). **i** Circular reconstructed image with the largest diameter. **j** Range in which the magnified object light pulse propagates on the image plane

7 Conclusions

In this study, to evaluate the effects of difference in the sweeping speed of the light pulses, we developed and demonstrated the numerical simulation model of light-in-flight recording by holography with a magnifying optical system. The numerical simulation is based on the ray tracing method. We were able to qualitatively evaluate the reconstructed images by changing the speeds at which the light pulses sweep the recording material. We numerically simulated the magnified light pulse under the following conditions: when the sweeping speed of the object light pulse is faster than that of the reference light pulse, and when the sweeping speed of the object light pulse is equal to the reference light pulse. The simulation results showed that the distortions of the reconstructed images become larger when the sweeping speed of the object light pulse differs from that of the reference light pulse. In addition, the simulation results showed that the recording time of the motion picture is affected by the magnifying optical system. Besides, when introducing the magnifying optical system into light-in-flight recording by holography to observe the magnified light pulse, a compensation method for distortions is required to accurately observe the magnified images of the light pulse. Our study will contribute towards developing and optimizing an optical system of light-in-flight recording by holography to observe the magnified light pulse.

Supplementary Information The online version contains supplementary material available at https://doi.org/10.1007/s00340-022-07773-3.

Funding This work was partially supported by the Japan Society for the Promotion of Science (JSPS), KAKENHI Grant-in-Aid for Scientific Research (A) (17H01062), KAKENHI Grant-in-Aid for Transformative Research Areas (A) (20H05887), and KAKENHI Grant-in-Aid for JSPS Research Fellows (20J23542).

Data availability Data underlying the results presented in this paper are not publicly available at this time but may be obtained from the authors upon reasonable request.

Declarations

Conflict of interest The authors declare no conflicts of interest.

References

1. A.Y. Vorobyev, C. Guo, Laser Photon. Rev. **7**, 385 (2013)
2. S. Heuke, S. Sivankutty, C. Scotte, P. Stockton, R.A. Bartels, A. Sentenac, H. Rigneault, Optica **7**, 417 (2020)
3. X. Tsampoula, V. Garcés-Chávez, M. Comrie, D.J. Stevenson, B. Agate, C.T.A. Brown, F. Gunn-Moore, K. Dholakia, Appl. Phys. Lett. **91**, 053902 (2007)
4. A. Vogel, J. Noack, G. Hüttman, G. Paltauf, Appl. Phys. B **81**, 1015 (2005)
5. Y. Ihm, D.H. Cho, D. Sung, D. Nam, C. Jung, T. Sato, S. Kim, J. Park, S. Kim, M. Gallagher-Jones, Y. Kim, R. Xu, S. Owada, J.H. Shim, K. Tono, M. Yabashi, T. Ishikawa, J. Miao, D.Y. Noh, C. Song, Nat. Commun. **10**, 2411 (2019)
6. J. Liang, L.V. Wang, Optica **5**, 1113 (2018)
7. K. Kumagai, S. Hasegawa, Y. Hayasaki, Optica **4**, 298 (2017)
8. H. Nemoto, T. Suzuki, F. Kannari, Appl. Opt. **59**, 5210 (2020)
9. H. Gersen, T.J. Karle, R.J.P. Engelen, W. Bogaerts, J.P. Korterik, N.F. van Hulst, T.F. Krauss, L. Kuipers, Phys. Rev. Lett. **94**, 073903 (2005)
10. G. Gariepy, N. Krstajić, R. Henderson, C. Li, R.R. Thomson, G.S. Buller, B. Heshmat, R. Raskar, J. Leach, D. Faccio, Nat. Commun. **6**, 6021 (2015)
11. X. Wang, L. Yan, J. Si, S. Matsuo, H. Xu, X. Hou, Appl. Opt. **53**, 8395 (2014)
12. A. Velten, R. Raskar, D. Wu, A. Jarabo, B. Masia, C. Barsi, C. Joshi, E. Lawson, M. Bawendi, D. Gutierrez, A.C.M. Trans, Graph. **32**, 1 (2013)
13. N. Abramson, Opt. Lett. **3**, 121 (1978)
14. D.I. Staselko, Y.N. Denisyuk, A.G. Smirnov, Opt. Spectrosc. **26**, 413 (1968)
15. T. Kubota, Y. Awatsuji, Opt. Lett. **27**, 815 (2002)
16. A. Komatsu, Y. Awatsuji, T. Kubota, J. Opt. Soc. Am. A **22**, 1678 (2005)
17. T. Kubota, K. Komai, M. Yamagiwa, Y. Awatsuji, Opt. Express **15**, 14348 (2007)
18. T. Inoue, A. Matsunaka, A. Funahashi, T. Okuda, K. Nishio, Y. Awatsuji, Opt. Lett. **44**, 2069 (2019)
19. T. Inoue, M. Sasaki, K. Nishio, T. Kubota, Y. Awatsuji, Appl. Opt. **60**, B59 (2021)
20. B. Nilsson, T.E. Carlsson, Appl. Opt. **37**, 7954 (1998)
21. J. Pomarico, U. Schnars, H.-J. Hartmann, W. Jüptner, Appl. Opt. **34**, 8095 (1995)
22. H. Rabal, J. Pomarico, R. Arizaga, Appl. Opt. **33**, 4358 (1994)
23. T. Kakue, K. Tosa, J. Yuasa, T. Tahara, Y. Awatsuji, K. Nishio, S. Ura, T. Kubota, IEEE, J. Sel. Top. Quantum. Electron. **18**, 479 (2012)
24. T. Kakue, M. Makino, M. Aihara, A. Kuzuhara, Y. Awatsuji, K. Nishio, S. Ura, T. Kubota, Jpn. J. Appl. Phys. **48**, 09LD01 (2009)
25. T. Kakue, N. Takada, T. Shimobaba, T. Ito, OSA Continuum **4**, 437 (2021)